



0735-1933(95)00010-0

## NUMERICAL MODELS FOR THE SIMULATION OF THE SIMULTANEOUS HEAT AND MASS TRANSFER DURING FOOD FREEZING AND STORAGE

A.M. Tocci<sup>1</sup> and R.H. Mascheroni<sup>2</sup>

CIDCA (Centro de Investigación y Desarrollo en Criotecnología de Alimentos)  
Universidad Nacional de La Plata - CONICET. La Plata (1900), ARGENTINA

<sup>1</sup> Comisión de Investigaciones Científicas de la Provincia de Buenos Aires

<sup>2</sup> Facultad de Ingeniería, Universidad Nacional de La Plata

(Communicated by J.P. Hartnett and W.J. Minkowycz)

### ABSTRACT

A numerical model was developed for the prediction of simultaneous heat and mass transfer during food freezing and storage. The resultant system of coupled partial differential equations, with time-varying coefficients was solved by two explicit finite-differences methods, one with constant mesh size and the other with equal volume elements. The prediction method was applied to the calculation of profiles of temperature and water content, and to the calculation of freezing times and weight losses under industrial freezing conditions, for spherical products such as meat balls and others.

### Introduction

Simultaneous heat and mass transfer during freezing of high-water content systems like foods, soils and biological materials represents a phenomenon of both academic and practical significance.

In the specific case of foodstuffs, the weight loss due to sublimation during freezing and subsequent frozen storage is an important economic and quality factor. Water loss produces changes in food overall appearance, colour, texture and taste. Besides, weight loss implies an equivalent economic loss. In this regard it is important to be able to predict the influence of process conditions on water vapour transfer between the foodstuff and the surrounding medium (air). In spite of its importance, weight losses have seldom been modelled in deep. Chau et al [1] and Chau and Gaffney [2] worked on simultaneous heat

and mass transfer during the refrigeration of respiring vegetables; Sukhwai and Aguirre-Puente [3] and Aguirre-Puente and Sukhwai [4] measured and modelled ice sublimation from frozen dispersed media. Most of the remaining published reports are based only on experimental data or on semiempirical models. The main difficulties for a detailed modelling are the coupling of mass and heat balances and the strong dependence of food thermophysical properties (thermal conductivity  $k$ , apparent heat capacity  $C_p$ , density  $\rho$  and water diffusion coefficient  $D$ ) with temperature in the freezing zone. An additional problem is the measurement or prediction of  $k$ ,  $C_p$  and  $D$  values in the partially dried surface layer of the frozen food.

### Mathematical Formulation

The spherical geometry was selected for the development of the model because it represents many important foods, e.g. : meat balls, whole fruits, melon portions and croquettes.

The energy balance to be solved is

$$\rho C_p \frac{\partial T}{\partial t} = \nabla(k \nabla T) \quad (1)$$

in which  $T$  is temperature,  $t$  time and, as previously stated,  $\rho$ ,  $C_p$  and  $k$  are functions of temperature and composition (Sanz et al [5]).

The apparent heat capacity  $C_p$  includes the true heat capacity and the enthalpy of fusion of ice. As most foods behave as a solution, the enthalpy of fusion is released over a wide temperature range and there are a freezing point depression and an equilibrium temperature-concentration curve.

The boundary conditions usual for this situation, are those of the sphere centre

$$\left. \frac{\partial T}{\partial r} \right|_{r=0} = 0$$

and sphere surface

$$-k \left. \frac{\partial T}{\partial r} \right|_{r=R} = h(T - T_a) + K L_v (C - C_a) \Big|_{r=R}$$

In these equations  $r$  is the radial coordinate and  $C$  the water concentration, while  $T_a$  and  $C_a$  refer to room air conditions. The symbol  $L_v$  is the heat of sublimation of ice.

For the heat ( $h$ ) and mass transfer coefficients ( $K$ ), their values were taken from our own data (Tocci and Mascheroni [6]) for belt freezers. They were corrected for the presence of a dehydrated surface layer of depth  $\delta$ . The layer thickness increases continuously with time and it depends on the heat transfer conditions, on the structure of the partially dehydrated food (mainly spatial arrangement of fibers and fat content) and on the adsorption isotherm of the food. The latter is, in turn, dependent on both air temperature and humidity [7]. The above-mentioned factors determine  $k_d$  and  $De_{eff}$  values, which can

have a wide range of variation [8].

$$h = \frac{h_0}{1 + \delta \frac{h_0}{k_d}} \quad K = \frac{K_0}{1 + \delta \frac{K_0}{Deff}}$$

In the resultant expressions for  $h$  y  $K$ , the symbols  $h_0$  and  $K_0$  correspond to the "nondehydrated" food;  $k_d$  is the thermal conductivity of the dehydrated food and  $Deff$  the diffusion coefficient of water vapour in the dehydrated solid matrix (Pham and Willix [8]).

Simultaneously, the mass balance to be solved is:

$$\frac{\partial C}{\partial t} = \nabla(D \nabla C) \quad (2)$$

Similar assumptions to those used in the development of the heat balance were done. The boundary conditions at food centre and surface are

$$\frac{\partial C}{\partial r} = 0 \Big|_{r=0}$$

$$-D \frac{\partial C}{\partial r} \Big|_{r=h} = K (C - C_a) \Big|_{r=R}$$

### Numerical Methods

Cleland and Earle [9] have shown that, during the modelling of food freezing through the numerical solution of Equation (1), similar results were obtained using either explicit finite-differences approaches or more elaborate two- or three-level implicit finite-differences schemes, provided sufficiently small time and space grid increments are used. The main source of errors are the values of thermal properties of foods used in the numerical method [9]. Based on these criteria, two explicit methods which differ in the spatial distribution of volume elements (and, consequently, of grid points), were tested.

#### Method A: Space increments of equal thickness

The symbols  $\Delta r$  and  $\Delta t$  are the radial and time increments, respectively. The distance step was defined as  $\Delta r = R/(I-1)$ . The time was defined as the product of the number of time steps and the time step value, or  $t = n\Delta t$ . The symbol  $T_i^n$  refers to a temperature calculated at  $r = (i-1)\Delta r$  and  $t = n\Delta t$ . The discretized formulation of the energy balance is given by Equation (3). After rearrangement, the general formulation valid for interior points of the food was obtained (Equation (4)). For the latter equation, the REL1 group was defined as:  $REL1 = \Delta t / \Delta r^2$ , and  $\alpha$  as  $\alpha = k / (\rho C_p)$ .

Specific expressions for system boundaries (centre ( $i=1$ ) and surface ( $i=I$ )) were developed by using the boundary conditions. They are as follows:

$$\rho_i^n C P_i^{n+1} \frac{(T_i^{n+1} - T_i^n)}{\Delta t} = \frac{k_i^n}{\Delta r^2} (T_{i+1}^n - 2 T_i^n + T_{i-1}^n) + \frac{(k_{i+1}^n - k_{i-1}^n) (T_{i-1}^n - T_{i-1}^n)}{4 \Delta r^2} + \frac{k_i^n}{(i-1) \Delta r^2} (T_{i+1}^n - T_{i-1}^n) \tag{3}$$

$$T_i^{n+1} = T_i^n + REL1 \alpha_i^n (T_{i+1}^n - 2 T_i^n + T_{i-1}^n) + REL1 \alpha_i^n (T_{i+1}^n - T_{i-1}^n) + \frac{REL1}{4 C P_i^n \rho_i^n} (k_{i+1}^n - k_{i-1}^n) (T_{i-1}^n - T_{i-1}^n) \tag{4}$$

$$T_1^{n+1} = T_1^n + 6 REL1 \alpha_1^n (T_2^n - T_1^n) \tag{5}$$

$$T_T^{n+1} = T_T^n + 2 REL1 \alpha_T^n [T_{T-1}^n - T_T^n] - 2 REL1 \frac{\Delta r}{k_T^n} (h (T_T^n - T_a) + K (C_T^n - C_a) L V) (1 + \frac{k_{T+1}^n - k_T^n}{4 k_T^n} + \frac{1}{I-1}) \tag{6}$$

Similar relations to Equations (4), (5) and (6) were obtained for  $C_i^{n+1}$ .

**Method B: Equal volume increments**

Chau and Gaffney [2] presented a detailed explanation of the method development. In brief, it consists of the division of the body (sphere or cylinder) into I concentric shells of equal volume  $\Delta V$ , where  $\Delta V = V / I$ , being V the total body volume. The main advantage of this method is that, for spheres and infinite cylinders, a higher "density" of grid points is obtained near the surface thus allowing for a more accurate calculation of temperature and concentration profiles. This is particularly important for the point located at the sphere surface since there is no mass associated to it. Therefore, the calculation of temperature can be made with higher accuracy [2].

Up to now, we have used this method only for the case of a sphere. In it, each grid point is located in the centre of the corresponding volume increment. The general formulation, based on an energy balance over a volume element  $\Delta V_i$  is given by Equation (7) which, rearranged, leads to Equation (8)

$$\rho_i^n C P_i^n \Delta V_i \frac{(T_i^{n+1} - T_i^n)}{\Delta t} = \frac{k_{i-\frac{1}{2}}^n A_{i-1}}{\Delta r_{i-1}} (T_{i-1}^n - T_i^n) - \frac{k_{i+\frac{1}{2}}^n A_i}{\Delta r_i} (T_i^n - T_{i+1}^n) \tag{7}$$

with:  $A_i = 4 \pi r_i r_{i+1}$  ;  $r_i = (1 + (1.5 - i) / I)$  for  $2 \leq i \leq I+1$  ;  $\Delta r_i = r_i - r_{i+1}$  ;  $\Delta r_{i-1} = r_{i-1} - r_i$ .

Point 1 is on the surface and Point I+2 is on the centre.

$$T_i^{n+1} = T_i^n \left[ 1 - \frac{\Delta t}{\Delta V_i \rho_i^n C p_i^n} \left( \frac{k_{i-\frac{1}{2}}^n A_{i-1}}{\Delta r_{i-1}} + \frac{k_{i+\frac{1}{2}}^n A_i}{\Delta r_i} \right) \right] + \frac{\Delta t}{\Delta V_i \rho_i^n C p_i^n} \left( \frac{k_{i-\frac{1}{2}}^n A_{i-1} T_{i-1}^n}{\Delta r_{i-1}} + \frac{k_{i+\frac{1}{2}}^n A_i T_{i+1}^n}{\Delta r_i} \right) \tag{8}$$

For  $i = 1$  (surface) a specific relation is deduced using the boundary condition as:

$$T_1^{n+1} = \frac{\left[ k_{3/2}^n \frac{A_1}{\Delta r_1} T_2^n + 4 \pi R^2 h T_a - 4 \pi R^2 K L v (C_1^n - C_a) \right]}{k_{3/2}^n \frac{A_1}{\Delta r_1} + 4 \pi R^2 h} \tag{9}$$

Point 1+2 is not calculated and may be obtained by polynomial extrapolation. This is a difficult problem to resolve during the phase change because profiles are approximately flat near the centre. Extrapolation can lead to the prediction of temperature values much higher than real ones. This possible source of errors has a great influence in the calculation of freezing times.

Relations similar to Equations (8) and (9) are obtained for  $C_1^{n+1}$ .

**Results**

The numerical methods were codified in QuickBASIC and the resultant simulation programs run on a PC AT 486. In all calculations, thermal properties of minced beef were used [5]. These properties depend of composition and temperature and have different prediction formulae for temperatures above and below the initial freezing point,  $T_{cr}$ .

Only one body size was tested:  $R = 0.019m$ . Three air temperatures  $T_a = -25, -30$  and  $-35^\circ C$  and air velocities values ranging from  $v_a = 1 \text{ m s}^{-1}$  to  $v_a = 10 \text{ m s}^{-1}$  were used. According to design, continuous belt freezers can have airflow parallel to the belt or through circulation. In the latter case the airflow can be either upwards or downwards. The three options were modelled to study the influence of this design variable on both the freezing time and weight loss. In all cases the relative humidity of air was 100% (saturation).

For Method A, 16 grid points were used in most calculations, although 31 and 46 grid points were also tested without meaningful differences in results. For 16 grid points  $\Delta t = 0.50 \text{ s}$  gave stable results.

For Method B, 14 volume elements were used in the calculations, but also 29 and 44 elements were tested without significant differences in the predicted freezing times (ft) or weight loss (wl). For  $I = 14$ ,  $\Delta t = 0.10 \text{ s}$  gave stable results.

There were no differences between predicted ft or wl of both methods. The highest difference in ft

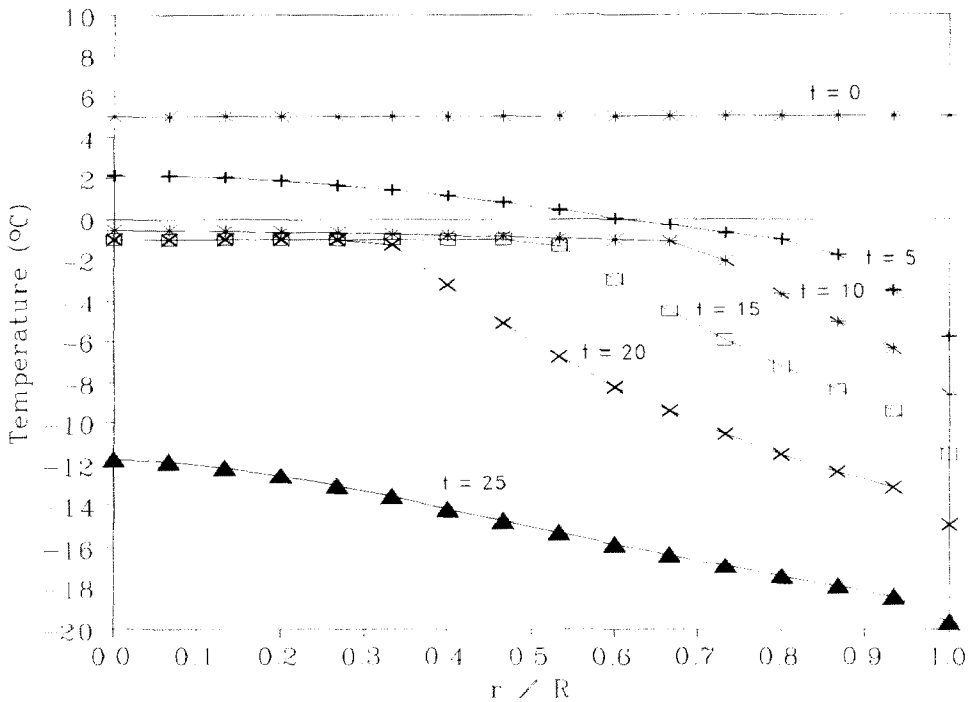


**FIG. 1**

**Predicted temperature profiles for the freezing of meat balls in belt freezer with  $T_i = 5^\circ\text{C}$ ,  $T_a = -30^\circ\text{C}$ ,  $v_a = 7 \text{ m/s}$  and downward air flow**

was as small as 0.22 min for  $T_a = -35^\circ\text{C}$  and  $v_a = 10 \text{ m s}^{-1}$ . For  $w$  the highest difference was 0.026% for  $T_a = -35^\circ\text{C}$  and  $v_a = 7 \text{ m s}^{-1}$ , in both cases for upward airflow through the belt.

As an example of the information obtained with the predictive method, Figure 1 shows the variation of temperature profiles with time. They were predicted for a meat ball undergoing freezing at the following operating conditions:  $T_i = 5.0^\circ\text{C}$ ,  $T_a = -30.0^\circ\text{C}$ ,  $v_a = 7.0 \text{ m s}^{-1}$  and downward airflow in through circulation, whose  $t_f$  was 26.74 min. A relevant feature is that, as long as freezing is in progress, the shape of temperature profiles becomes distorted near the surface. Such a distortion is caused by the formation of a layer of dehydrated tissue as a consequence of sublimation. This layer has different thermal properties and therefore it modifies both the heat capacity and the thermal conductivity.

On the other hand, Figure 2 exhibits the thermal history for three points (surface ( $r = R$ ), centre ( $r = 0$ ) and a position midway between both ( $r = 0.5 R$ )). The operating conditions are as in Figure 1. From the information presented in both figures, it can be noticed that the temperatures at, or very near the surface, rapidly fall below the initial freezing point  $T_{cr}$ , while, as long as inner points are considered,

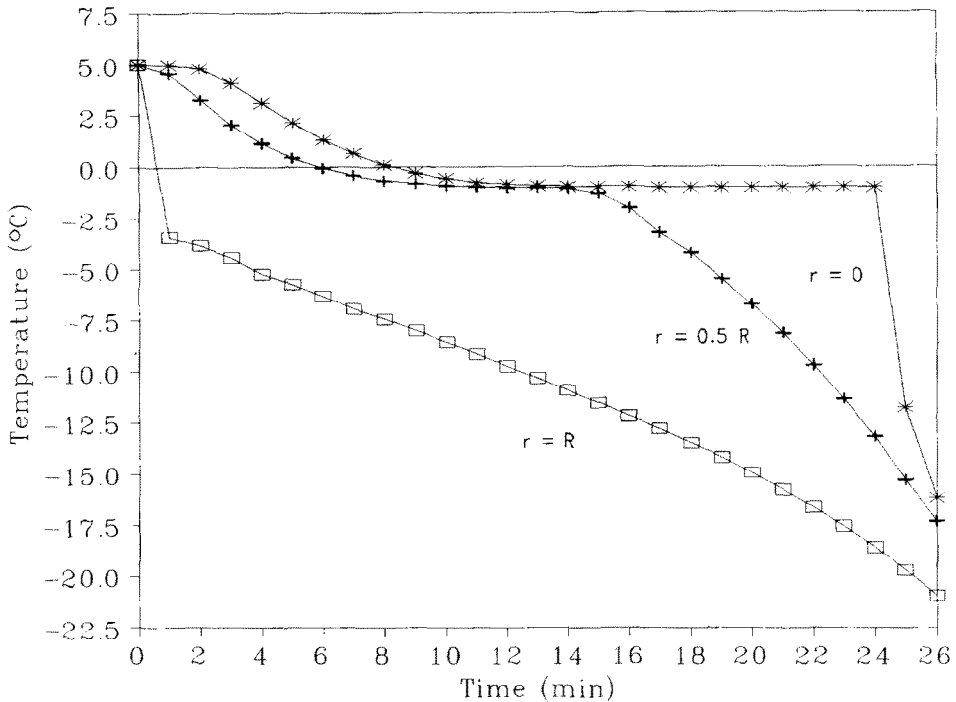


**FIG. 2**  
**Predicted temperature histories for different points of a meat ball during freezing**

there is an increasingly long period of time in which the temperature remains at  $T_{cr}$  (plateau). The duration of the plateau depends on both the composition and body size, and on heat transfer conditions ( $h$ ,  $T_a$ ).

Figure 3 shows the variation in predicted  $t_f$  (the time required to reach  $-18^\circ\text{C}$  in the centre) as a function of air temperature and velocity. As expected  $t_f$  is strongly dependent on both parameters and decreases with lower values of  $T_a$  and with the increase of  $v_a$ .

Figure 4 presents the data of  $w_l$  for the same operating conditions. Predicted  $w_l$  range between 1.04 and 2.07% for extreme values of  $T_a$  and  $v_a$ . These results show the possibility of reducing water losses through an adequate selection of freezing conditions.

Figure 5 presents the ratio of predicted freezing times with consideration of water evaporation to predicted freezing times with no consideration of mass transfer. From this Figure, an error ranging from 5 to 15% was detected when the effect of ice sublimation on freezing time was neglected.

Finally, Figure 6 presents a comparison between freezing times and weight losses predicted by the model for the three possible design cases of airflow direction with respect to the belt. As it can be

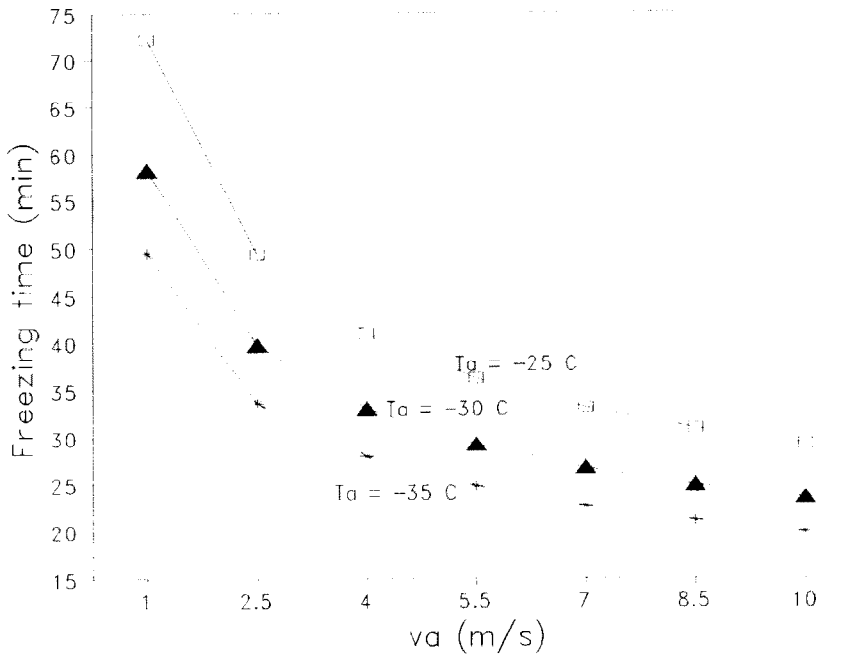


FIG. 3

**Predicted freezing times for meat balls in continuous belt freezers with upward air flow through the belt**

observed, the downward airflow in through circulation always led to the shortest freezing time and lowest weight loss, at equal remaining working conditions.

**Discussion and Conclusions**

- It is possible to predict simultaneous heat and mass transfer during food freezing and storage through the use of a theoretical model, with no simplifying assumptions, by employing a numerical solution based on explicit finite difference-methods. This facilitates the development and use of calculation programs.
- The developed model enables to calculate temperature and concentration profiles, freezing times and weight losses.
- The model can be used to improve equipment design in matters such as energy consumption and weight losses during the process.
- There were no significant differences between the results obtained with both numerical schemes tested.

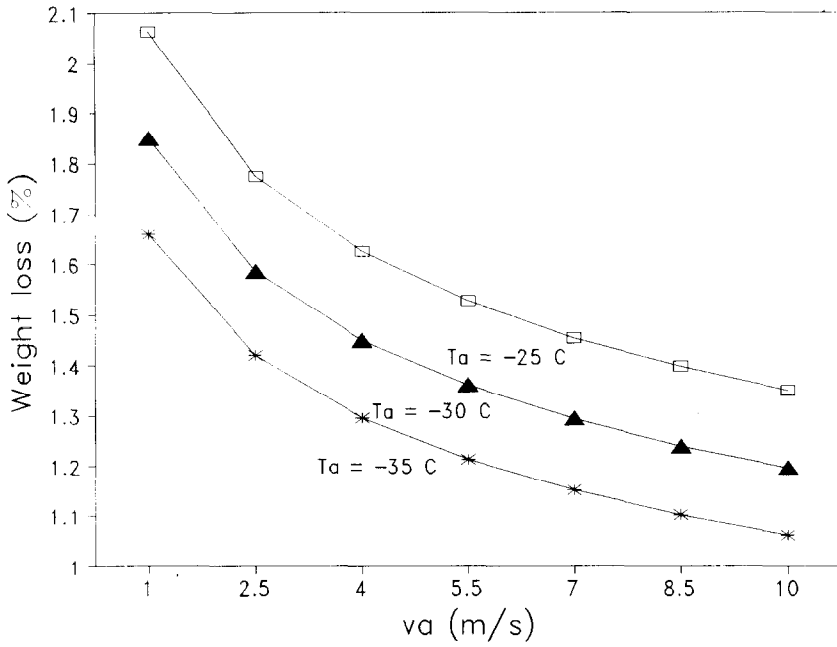


FIG. 4

Predicted weight losses during the freezing of meat balls in belt freezers

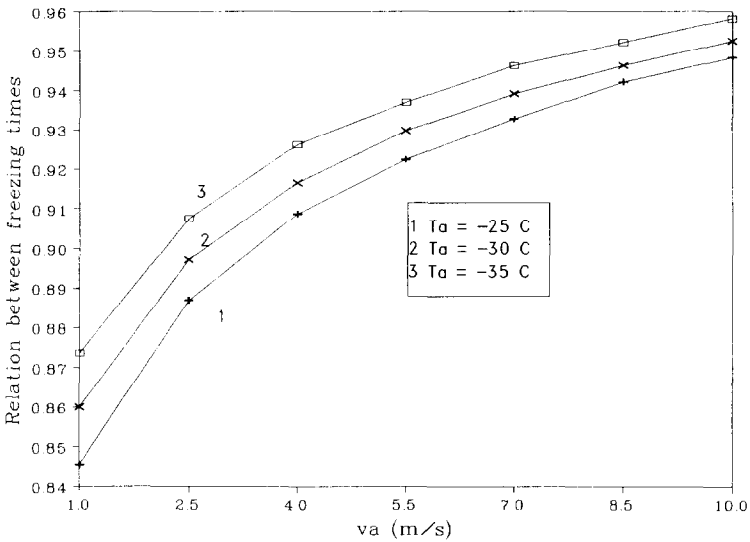
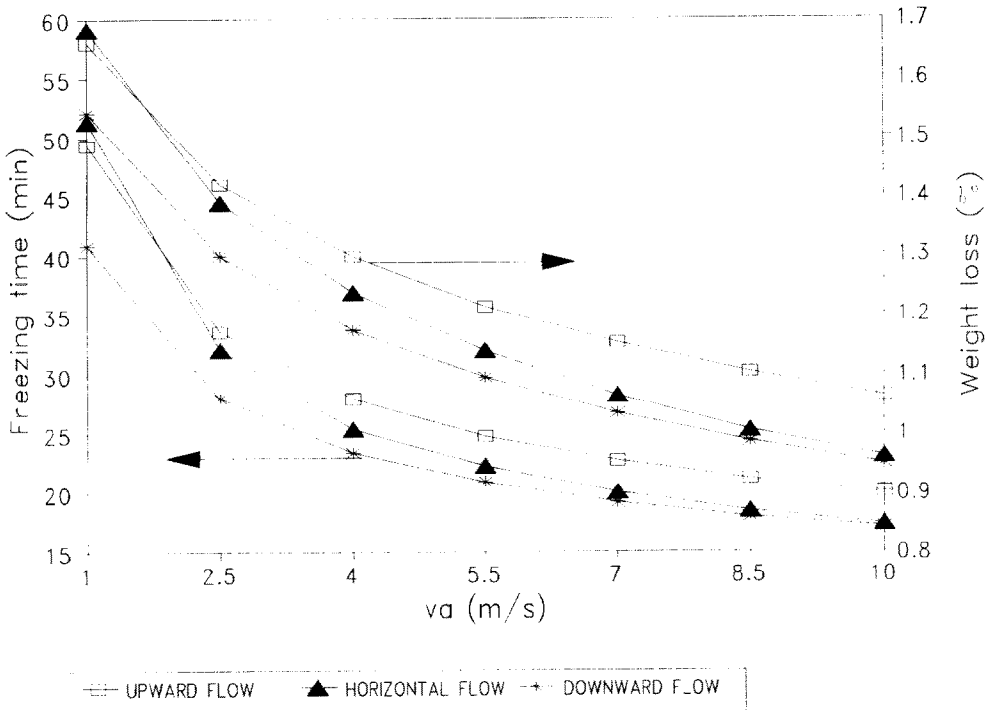


FIG. 5

Relation between predicted freezing times with and without considering ice sublimation



**FIG. 6**  
**Predicted freezing times and weight losses for different types of air flow**

#### References

1. K.V. Chau, J.J. Gaffney and R.A. Romero, *ASHRAE Trans.* **94**, 1541 (1988).
2. K.V. Chau and J.J. Gaffney, *J. Food Sci.* **55**, 484 (1990).
3. R.N. Sukhwai and J. Aguirre-Puente, *Rev. Gén. Therm. Fr.* (262), 663 (1983).
4. J. Aguirre-Puente and R.N. Sukhwai, *Proceedings of The Third International Offshore Mechanics and Arctic Engineering Symposium*, Vol. 3, p. 38, V. Lunardini (1983).
5. P.D. Sanz, M. Domínguez Alonso and R.H. Mascheroni, *Lat. Am. Appl. Res.* **19**, 155 (1989).
6. A.M. Tocci and R.H. Mascheroni, *J. Food Engng.* (in press), 1994.
7. I.G. Chumak and P.V. Sibiriakov, *Izv. Vuzov Pisch. Tejn.* (2), 54 (1988).
8. Q.T. Pham and J. Willix, *J. Food Sci.* **49**, 1275 (1984).
9. A.C. Cleland and R.L. Earle, *J. Food Sci.* **49**, 1034 (1984).

*Received September 13, 1994*